

Computational Study of the Effect of Finger Width and Aspect Ratios for the Electrostatic Levitating Force of MEMS Combdrive

Shiang-Woei Chyuan, Yunn-Shiuan Liao, *Member, ASME*, and Jeng-Tzong Chen

Abstract—Since the width ratio between movable and fixed fingers, and the aspect ratio between the height and width of fingers, can play very important roles for combdrive levitation control, computational study of variations in those parameters for electrostatic levitating force acting on the movable finger is indispensable for MEMS performance. For diverse finger width and aspect ratios of MEMS combdrive design, the BEM has become a better method than the domain-type FEM because BEM can provide a complete solution in terms of boundary values only, with substantial saving in modeling effort. DBEM still has some advantages over conventional BEM for singularity, so the DBEM was used to simulate the fringing of field around the edges of the fixed finger and movable finger of MEMS combdrive for diverse finger width and aspect ratios. Results show that the less the finger width ratio is, the larger the levitating force acting is. Furthermore, the levitating force becomes more dominant as the aspect ratio increases, but it will be kept constant while the aspect ratio becomes larger. [1233]

Index Terms—Aspect ratio, combdrive, DBEM, finger width ratio, levitating force, MEMS.

I. INTRODUCTION

MEMS (microelectromechanical systems) combdrive usually has two sets of fingers, the one which is connected to the substrate is called fixed fingers (or stationary electrode), and the other which is released from the substrate is called movable fingers (see Fig. 1). When two different voltages are applied to these two sets of fingers, the resulting electrostatic force drives the movable fingers toward the fixed ones. Thus, motion is produced by this combdrive in the direction of the movement of the movable fingers [1]. Because combdrive can be designed for either electrostatic actuator or capacitive sensing, it has become a very important device in MEMS [2]. Basically, the in-plane interdigitated combdrives are used in in-plane or small out-of-plane/torsional motions [3], and the asymmetric combdrives can be utilized to generate large out-of-plane or torsional motions [4]. Generally speaking, in a typical in-plane interdigitated combdrive, the capacitance is linear with displace-

ment, resulting in an electrostatic driving force, which is independent of the position of the movable fingers except at the ends of the range of travel [5]. But for some special applications, combdrive with variable-gap profiles can be designed that will deliver desired driving force profiles by solving an appropriate inverse problem [6]. Even though surface-micromachined polysilicon resonators, which are driven by interdigitated capacitors, have several attractive properties published in [2], it is essential that both movable finger and fixed finger of combdrive remain coplanar for high-quality MEMS devices. Because the levitation effect will seriously downgrade the performance and reliability of MEMS devices, how to obtain the actual electrostatic force responsible for levitation plays a very important role. As a result, knowledge of the electric potential V and electric field intensity E around fixed finger, movable finger and ground plane of MEMS under diverse values of finger width and aspect ratios for combdrive considering the fringing of field around the edges are very important for engineers because the levitating force acting on the movable finger is obviously dependent on the electrostatic field [7]. Therefore, the main goal of this article is to search for an efficient method to investigate the effect of finger width and aspect ratio variation for the levitation of MEMS combdrive.

Basically, electrical engineers are familiar with electrostatic problems, and diverse numerical methods have been regularly used in MEMS and EM (electromagnetics). Among diverse numerical approaches, finite element method (FEM), which is based on the representation and approximate solution of boundary value problems of engineering mathematics in terms of partial differential equations [8], [9], and boundary element method (BEM) based on integral equations [10] have moved from being research tools for scientists to become powerful design tools for engineers. One of the main advantages of BEM, when compared to FEM, is that discretizations are restricted only to the boundaries, making data generation much easier. The BEM is also ideally suited to the analysis of external problems where domains extend to infinity, since discretizations are confined to the internal boundaries with no need to truncate the domain at a finite distance and impose artificial boundary conditions, and to problems involving some form of discontinuity or singularity, due to the use of singular fundamental solutions as test functions. It is also interesting to point out that the unknowns in BEM are a mixture of the potential and its normal derivative, rather than the potential only as in FEM. This is a consequence of the BEM being a “mixed” formulation, and constitutes an important advantage

Manuscript received December 30, 2003; revised August 3, 2004. Subject Editor N. de Rooij.

S.-W. Chyuan was with the Graduate Institute of Mechanical Engineering, National Taiwan University, Taipei, Taiwan, R.O.C. He is now with Chung Shan Institute of Science and Technology, Lung-Tan, Tao-Yuan 325, Taiwan, R.O.C. (e-mail address: yeaing@iris.seed.net.tw).

Y.-S. Liao are with the Graduate Institute of Mechanical Engineering, National Taiwan University, Taipei, Taiwan, R.O.C.

J.-T. Chen is with the Department of Harbor and River Engineering, National Taiwan Ocean University, Keelung, Taiwan, R.O.C.

Digital Object Identifier 10.1109/JMEMS.2004.839031

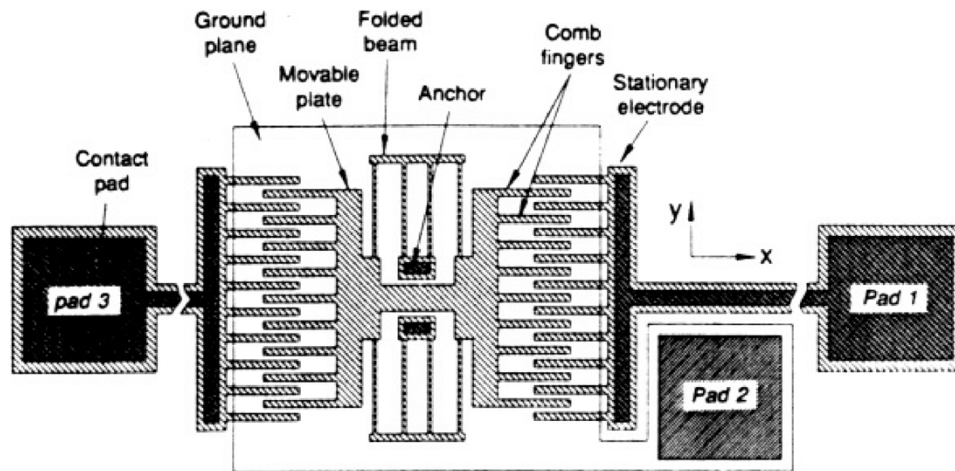


Fig. 1. Layout of a linear lateral resonator driven and sensed with interdigitated capacitors (electrostatic combdrive). [1].

over FEM. Especially for diverse values of finger width and aspect ratios for MEMS combdrive, many laborious works of FEM compared with those of BEM are needed because BEM can provide a complete solution in terms of boundary values only, with substantial saving in modeling effort. Therefore, there is no doubt that BEM has become a very appealing approach in numerical simulation of MEMS [11] even if many engineers still use commercial package to set up diverse FEM models during the variable design stage today.

The paper is organized as follows. Section II involves the comparison between dual BEM (DBEM) with conventional BEM. In Section III, we concisely introduce the procedure of DBEM for electrostatic problems. Numerical results are provided and compared in Section IV to establish the validity and accuracy of the DBEM and to study the effect of finger width and aspect ratio variation for the levitation of MEMS combdrive. Some remarks based on the reported results were discussed in Section V. Finally, there is a concise conclusion in Section VI.

II. COMPARISON BETWEEN DBEM WITH CONVENTIONAL BEM

Because modern MEMS and electron device design usually contains very thin conducting plates (e.g., a parallel-plate capacitor), the singularity problems arising from a degenerate boundary (The degenerate boundary refers to a boundary, two portions of which approach each other such that the exterior region between the two portions becomes infinitely thin [12]) are frequently formed, and it is well known that the coincidence of the boundaries gives rise to an ill-conditioned problem. The sub-domain technique in conventional BEM with artificial boundaries for degenerate boundary has been introduced to ensure a unique solution. The main drawback of the technique is that the deployment of artificial boundaries is arbitrary and, thus, cannot be implemented easily into an automatic procedure. In addition, model creation is more troublesome than in the single domain approach. To tackle such degenerate boundary electrostatic problems, DBEM has been proposed in [13], and all the above-mentioned boundary value problems

can be solved efficiently in the original single domain if using DBEM.

Although there is no singularity arising from degenerate boundary for MEMS devices studied in this article, the DBEM still has some advantages [12] over conventional BEM. 1) An essential ingredient for all adaptive BEM is a reliable estimate of the local error. The hypersingular integral equation used in DBEM is a complementary equation available for error estimation. 2) The hypersingular integral equation of DBEM can be used to directly calculate the tangent electric field instead of using the numerical derivative of the obtained potential field. The tangent derivative along the boundary has been formulated in terms of both the boundary potential and the boundary normal flux. Therefore, the numerical error from conventional BEM facing the fringing of field around the edges could be eliminated. 3) In the coupling of FEM and BEM, the symmetry requirement of the stiffness matrix is especially useful. The four kernel functions in the dual integral equations display the elegant structure of potential theory. The symmetry and transpose symmetry properties for the four kernel functions of DBEM have been found. 4) In addition, for electrostatic problems with some specific geometry, another singularity caused by a degenerate scale will be encountered since the influence matrix is rank deficient, and numerical results become unstable. The hypersingular formulation of DBEM can also play a very important role for solving this singularity arising from rank deficient problem [14].

Even if some simplified numerical models for electrostatic combdrive can be found in [4], [5], there are still three types of fringing fields not taken into account, which result from the ground plane, widths and heights of fixed and movable fingers. In order to obtain more reasonable computational results for the electric field, the DBEM is employed and developed to analyze electrostatic problems for MEMS combdrive levitation considering the fringing of field around the edges in the article. After using DBEM to accurately calculate the electrostatic response of the comb finger biased with a dc voltage, the induced vertical force per unit length of the movable comb finger at different levitation positions can be obtained. Then this vertical force density can be plotted against levitation at different dc bias voltages like

[4], [5]. In order to check the validity of the numerical model presented in this article, an example of in-plane interdigitated combdrive designs from [3] is furnished, and the solutions of DBEM are compared with analytical solutions if available and with a commercial FEM package [15]. After the accuracy by way of DBEM was satisfied, the DBEM was used to study the finger width and aspect ratio variation for the levitating force of MEMS combdrive in the following section.

III. DUAL INTEGRATION EQUATION FOR ELECTROSTATIC PROBLEMS

For a homogeneous medium, the governing equation of electrostatics can be written in the following form

$$\nabla^2 V = -\frac{\rho}{\varepsilon} \quad (1)$$

where ∇^2 is the Laplacian operator. Equation (1) is known as Poisson's equation; it states that the divergence of the gradient of electric potential (V) equals $-\rho/\varepsilon$ for a simple medium, where ε is the permittivity of the medium and ρ is the volume density of free charges [7]. At points in a simple medium where there is no free charge, (1) is reduced to

$$\nabla^2 V = 0 \quad (2)$$

which is known as Laplace's equation. Equation (2) plays a very important role in MEMS and EM. It is the governing equation for electrostatic problems involving a set of conductors, such as capacitors, maintained at different potentials. Once V is found from (2), \mathbf{E} (electric field intensity) can be determined from $-\nabla V$, and the charge distribution on the conductor surfaces can be determined from $\rho_s = \varepsilon E_n$.

Generally the electrostatic problem consists of finding the unknown potential function Φ (or V) in the partial differential equation. In addition to the fact that Φ satisfies $\nabla^2 \Phi = 0$ within a prescribed solution region Ω , the potential function Φ must satisfy certain conditions on \mathbf{B} which is the boundary of Ω . Usually these boundary conditions are the *Dirichlet* ($\Phi(x) = f(x)$) and *Neumann* ($\partial\Phi(x)/\partial n_x = g(x)$) types, where $f(x)$ and $g(x)$ denote known boundary data, and n_x is the unit outer normal vector at the point x on the boundary \mathbf{B} . Therefore, the governing equation of electrostatic problems could be written in the following form:

$$\nabla^2 \Phi(x) = 0, \quad x \text{ in } \Omega. \quad (3)$$

Based on the dual boundary integral equation formulation for electrostatic problem [13], we have

$$\alpha\Phi(x) = \text{CPV} \int_{\mathbf{B}} T(\mathbf{s}, \mathbf{x}) \Phi(\mathbf{s}) d\mathbf{B}(\mathbf{s}) - \text{RPV} \int_{\mathbf{B}} U(\mathbf{s}, \mathbf{x}) \left[\frac{\partial\Phi(\mathbf{s})}{\partial n_{\mathbf{s}}} \right] d\mathbf{B}(\mathbf{s}) \quad (4)$$

$$\alpha \left[\frac{\partial\Phi(x)}{\partial n_x} \right] = \text{HPV} \int_{\mathbf{B}} M(\mathbf{s}, \mathbf{x}) \Phi(\mathbf{s}) d\mathbf{B}(\mathbf{s}) - \text{CPV} \int_{\mathbf{B}} L(\mathbf{s}, \mathbf{x}) \left[\frac{\partial\Phi(\mathbf{s})}{\partial n_{\mathbf{s}}} \right] d\mathbf{B}(\mathbf{s}) \quad (5)$$

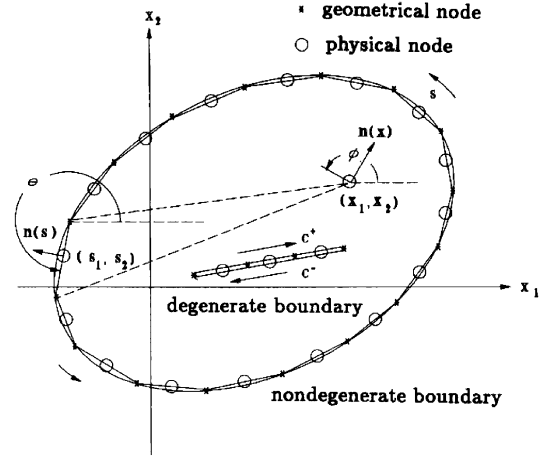


Fig. 2. Boundary element discretization for degenerate boundary and nondegenerate boundary.

where the kernel functions, $U(\mathbf{s}, \mathbf{x}) = \ln(r)$, $T(\mathbf{s}, \mathbf{x}) = \partial U(\mathbf{s}, \mathbf{x})/\partial n_{\mathbf{s}}$, $L(\mathbf{s}, \mathbf{x}) = \partial U(\mathbf{s}, \mathbf{x})/\partial n_{\mathbf{x}}$, $M(\mathbf{s}, \mathbf{x}) = \partial^2 U(\mathbf{s}, \mathbf{x})/\partial n_{\mathbf{x}} \partial n_{\mathbf{s}}$, $r = |\mathbf{s} - \mathbf{x}|$, \mathbf{s} , and \mathbf{x} being position vectors of the points s and x , respectively, and $n_{\mathbf{s}}$ is the unit outer normal vector at point s on the boundary (see Fig. 2). In addition, *RPV* is the *Riemann Principal Value*, *CPV* is the *Cauchy Principal Value*, *HPV* is the *Hadamard Principal Value*, and α depends on the collocation point ($\alpha = 2\pi$ for an interior point, $\alpha = \pi$ for a smooth boundary, $\alpha = 0$ for an exterior point). The commutativity property of the trace operator and the normal derivative operator provides us with alternative ways to calculate the Hadamard principal value analytically. Generally, (4) is called *singular boundary integral equation*, and (5) is called *hypersingular boundary integral equation*. Since the hypersingular boundary integral equation plays an important role in the degenerate problems, many researchers have paid much attention to this. After discretizing the boundary into $2N$ boundary elements, (4) and (5) reduce to

$$[U]_{2N \times 2N} \{t\}_{2N \times 1} = [T]_{2N \times 2N} \{u\}_{2N \times 1} \quad (6)$$

$$[L]_{2N \times 2N} \{t\}_{2N \times 1} = [M]_{2N \times 2N} \{u\}_{2N \times 1} \quad (7)$$

where $[U]$, $[T]$, $[L]$ and $[M]$ are the four influence matrices, $\{u\}$ and $\{t\}$ are the boundary data for the primary and the secondary boundary variables, respectively.

IV. DBEM SIMULATION FOR THE ELECTROSTATIC FIELD OF MEMS COMBDRIVE LEVITATION

The successful electrostatic actuation of micromechanical structures requires a ground plane under the structure in order to shield it from relatively large vertical fields [3]. In order to demonstrate the efficiency and suitability of DBEM presented in this article, an electrostatic combdrive problem proposed by Tang, Lim, and Howe [3] was used in the first case. In this case, a $4\text{-}\mu\text{m}$ -wide \times $2\text{-}\mu\text{m}$ -high comb finger excited by two identically sized electrodes situated $2\text{-}\mu\text{m}$ away from both sides of the finger, and $2\text{-}\mu\text{m}$ above a grounded substrate was used (see Fig. 1). The following case was used to study the effect of width ratio ($R_1 = w_m/w_f$) between movable and fixed fingers (from $1/4$ to 4) for levitation of MEMS combdrive (see Fig. 3),

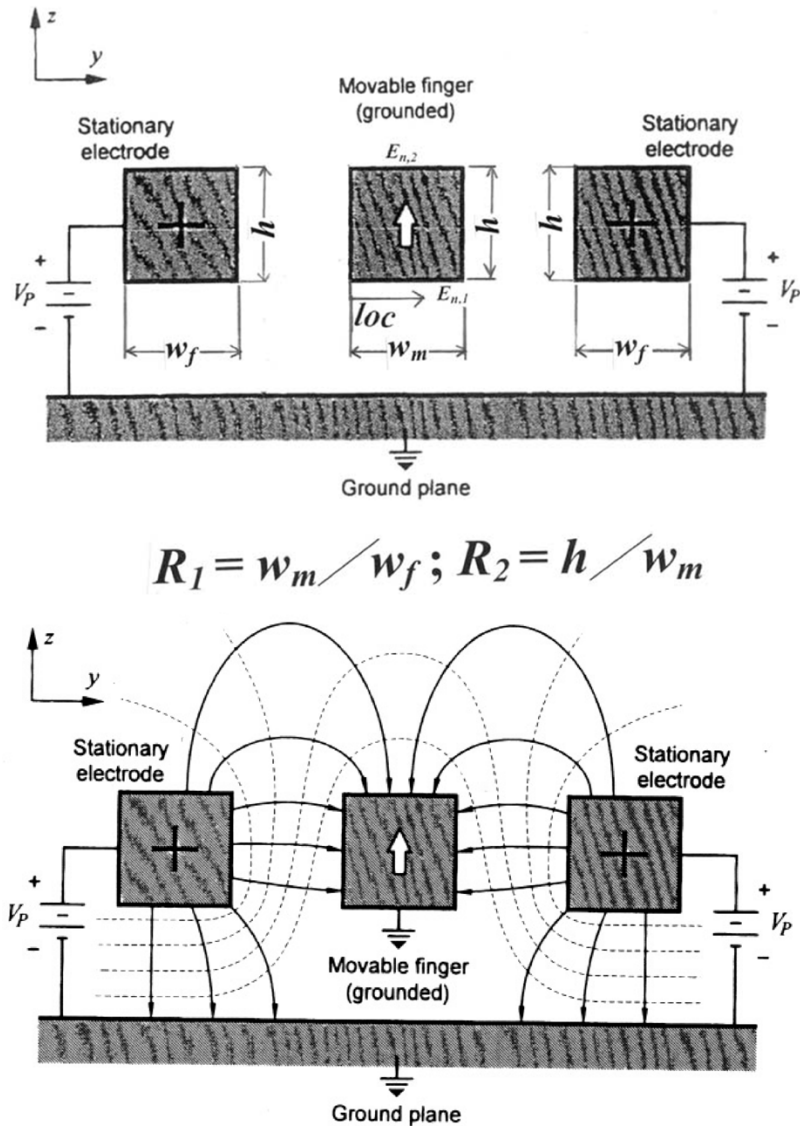


Fig. 3. Cross section of the potential contours (dashed lines) and the electric fields (solid lines) of a comb finger under levitation force induced by two adjacent electrodes biased at a positive potential. [3].

but the width of movable finger (w_m) is still kept $4.0 \mu\text{m}$. After that, we intend to investigate the effect of aspect ratio ($R_2 = h/w_m$) between the height h and width of fingers (from $1/4$ to 4), but the w_m and w_f are both still kept $4.0 \mu\text{m}$.

A. Case Study

A comb finger under levitation force induced by two adjacent electrodes biased at a positive potential V_p shown in Fig. 3. In order to check the accuracy if using DBEM, we will determine the electric potential distribution first.

From Fig. 3, one can see that there is an obvious fringing of field around the edges of fixed finger and movable finger, and the physical behavior (e.g., electric potential and electric field intensity) of this area is very complicated [3]. Since it is not easy to obtain the analytical solutions, and some simplified numerical models for electrostatic combdrives from [4], [5] can not accurately simulate the fringing field, the FEM simulation [15] was used to compare with the following DBEM data. Because of the

fringing of field around the edges, a large finite element model was set up in order to obtain a reasonable result. In addition, the symmetric boundary between two adjacent fingers using proper Neumann boundary condition was used to cut down the dimension of FEM and DBEM models.

Over three thousand points will be analyzed using coarse mesh discretization (95 elements and 95 nodes; see Fig. 4) of DBEM, and compared with reference data computed from a large refined mesh FEM model [3608 elements and 3790 nodes; see Fig. 5(a)] because the results from the coarser mesh FEM model [1490 elements and 1607 nodes; see Fig. 5(b)] are not adequately accurate. The results of electric potential for the same interior nodes between movable and fixed fingers under refined mesh FEM and coarse mesh DBEM were shown in Fig. 6. Comparing the results of electric potential field (equipotential lines) using coarse mesh DBEM and refined mesh FEM, one can see that the difference of electric potential distribution is very little, so the DBEM used in this article is an efficient method for solving electrostatic MEM combdrive problems. From Fig. 6,



Fig. 4. The related DBEM coarse mesh discretization.

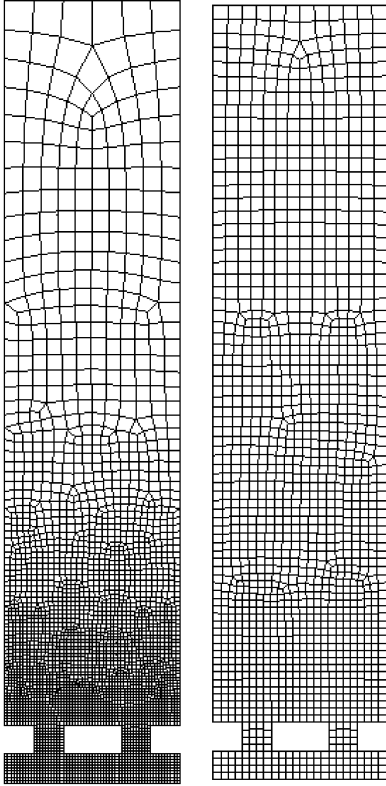
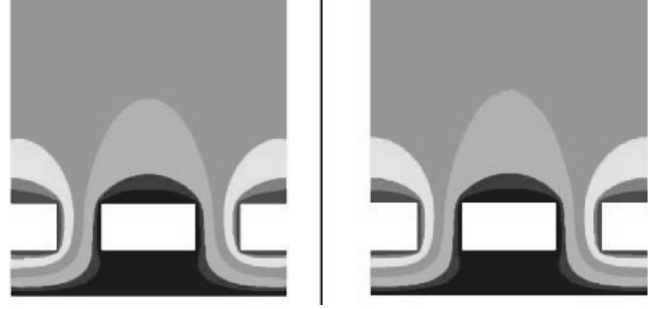
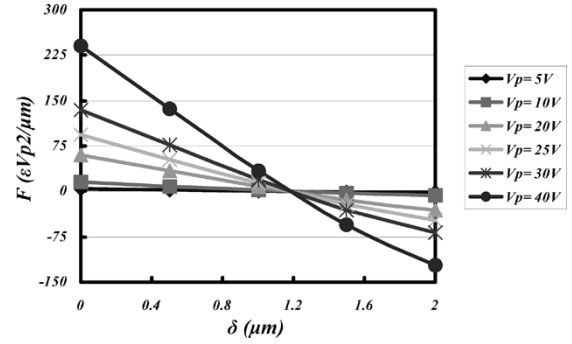


Fig. 5. The related FEM mesh discretization (Left side: Refined mesh model. Right side: Coarser mesh model).

the ground plane contributes to an obviously unbalanced electrostatic field distribution if a heavily doped polysilicon film underlies the resonator and the comb structure like Fig. 3.

Besides the results of electric potential field, the distribution of normal electric field intensity (E_n) on the bottom and upper side of movable finger can be obtained by way of DBEM. Because the charge distribution on the conductor surfaces can be


 Fig. 6. Results of electric potential field (equipotential lines — Red color: $+V_p$; Blue color: 0) of combdrive using coarse mesh DBEM (Left part) and refined mesh FEM (Right part).

 Fig. 7. The levitating force density (F) acting on the movable finger under diverse levitation (δ) and V_p .

determined from $\rho_s = \varepsilon E_n$ (The normal component of the electric field E_n at a conductor boundary is equal to the surface charge density ρ_s on the conductor divided by the permittivity ε [7]) if ε is a constant, the relationship between the normal force density f_n acting on the surface of a conductor and the charge density ρ_s of that conductor is

$$f_n = -0.5 \frac{\rho_s^2}{\varepsilon}. \quad (8)$$

Thus, the electrostatic force density F_n acting on the movable finger along the boundary

$$F_n = \int_{\mathbf{B}} f_n d\mathbf{B} \quad (9)$$

can be calculated if ρ_s (or E_n) is known. Therefore, the levitating force density F (normal to the substrate) acting on each movable finger is equal to the difference of electrostatic force density F_n between upper side and bottom of concerned movable finger, and that is obviously dependent on the difference of $E_{n,1}$ and $E_{n,2}$ shown in Fig. 3. Since the difference of $E_{n,1}$ and $E_{n,2}$ is obvious in this case, the imbalance in the field distribution will result in a net vertical force induced on the movable comb fingers, which levitates the structure away from the substrate. Calculated by (8) and (9), the value of F acting on the movable finger is $0.1504 \varepsilon V_p^2 / \mu\text{m}$ for this case. To go a step further, the F under diverse levitation (δ) and V_p can be shown in Fig. 7. There are some interesting results from Fig. 7 can be found. First, the stable equilibrium levitation, δ_0 , ($1.19 \mu\text{m}$ for this case), is the same for any nonzero bias voltages V_p . Hence, in the absence of a restoring spring force, the movable finger

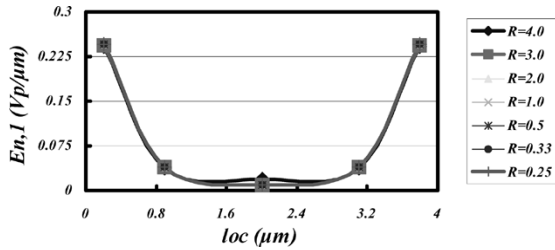


Fig. 8. The distribution of normal electric field intensity $E_{n,1}$ on the bottom side of movable finger under diverse values of R_1 and loc .

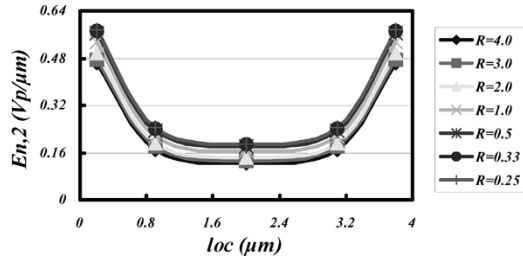


Fig. 9. The distribution of normal electric field intensity $E_{n,2}$ on the upper side of movable finger under diverse values of R_1 and loc .

will be levitated to δ_0 upon the application of a dc bias. Second, given any δ , the F is proportional to V_p^2 . In addition, the value of δ_0 from [3] is $1.22 \mu\text{m}$ for the same case, so the difference of δ_0 between DBEM and [3] is only 2.46%. Consequently, we can verify the computational accuracy of DBEM presented in this article.

Since the width ratio R_1 ($R_1 = w_m/w_f$) between movable and fixed fingers can play a very important role for the levitation of MEMS combdrive, the effect of this will be investigated in the following case. Similar to the aforementioned case, the w_m is still kept $4.0 \mu\text{m}$, but R_1 are variable from $1/4$ to 4 . If a movable comb finger when differential dc bias V_p is applied to the two adjacent electrodes shown in Fig. 3, let's determine the distribution of E_n on the bottom and upper sides of movable finger under diverse values of R_1 . Besides E_n , also calculate the F acting on the movable finger. As many FEM models need to be established for diverse R_1 variation, domain-type FEM is not a good choice for this case, and we use DBEM to perform the following tasks since the discretizations of DBEM are restricted only to the boundaries, making data generation much easier than FEM. By way of the DBEM, the distribution of E_n on the bottom and upper sides of movable finger under diverse values of R_1 were shown in Figs. 8 and 9 respectively. From Fig. 9, one can see that the values of $E_{n,2}$ on the upper side of movable finger are obviously dependent on the values of R_1 and the location to the left side of movable finger (loc). Unlike $E_{n,2}$, the values of $E_{n,1}$ on the bottom side of movable finger are only apparently counting on the value of loc , and the effect of the values of R_1 can be ignored (see Fig. 8). Because the difference of F_n between the upper and bottom sides of concerned movable finger is obvious under diverse values of R_1 , the F acting on the movable finger shown in Fig. 10 does apparently rely on the variation of R_1 if the w_m is still kept $4.0 \mu\text{m}$. Results also show that the less the R_1 is, the larger the F is.

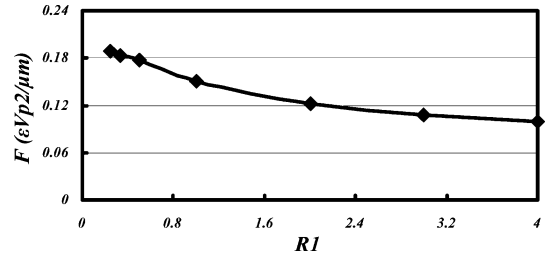


Fig. 10. The levitating force density (F) acting on the movable finger under diverse R_1 .

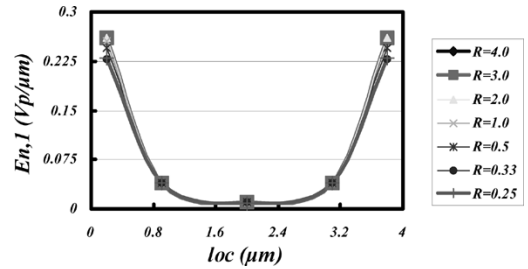


Fig. 11. The distribution of $E_{n,1}$ on the bottom side of movable finger under diverse values of R_2 and loc .

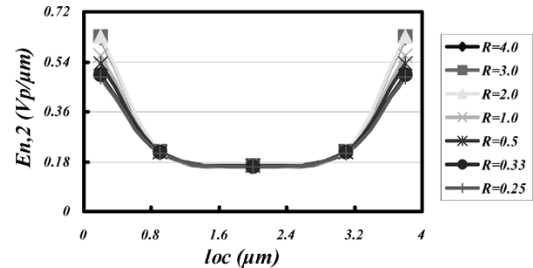


Fig. 12. The distribution of $E_{n,2}$ on the upper side of movable finger under diverse values of R_2 and loc .

As we know, the F is a strong function of aspect ratio R_2 ($R_2 = h/w_m$) between the height and width of fingers as well as R_1 . In this case, the values of R_2 are variable from $1/4$ to 4 , but the w_m and w_f are both still kept $4.0 \mu\text{m}$ and a movable comb finger when differential dc bias V_p is also applied to the two adjacent electrodes shown in Fig. 3, let's calculate the distribution of E_n on the bottom and upper sides of movable finger under diverse values of R_2 , and also calculate the F acting on the movable finger. By way of the DBEM, the distribution of E_n on the bottom and upper sides of movable finger under diverse values of R_2 were shown in Figs. 11 and 12 respectively. From Figs. 11 and 12, one can see that the fringing values of $E_{n,1}$ on the bottom and $E_{n,2}$ on the upper side of movable finger are both obviously dependent on the values of R_2 and loc , but the effect of R_2 on other areas is not apparent. Because the difference of F_n between the upper and bottom sides of concerned movable finger is also notable under diverse values of R_2 if R_2 is less than 2, the F acting on the movable finger shown in Fig. 13 does apparently rely on the variation (from $1/4$ to 2) of R_2 if the w_m and w_f are both still kept $4.0 \mu\text{m}$. Results also show that the F becomes more dominant as the value of R_2 increases from $1/4$ to 2 , but it will be kept constant while the R_2 is larger than 2 .

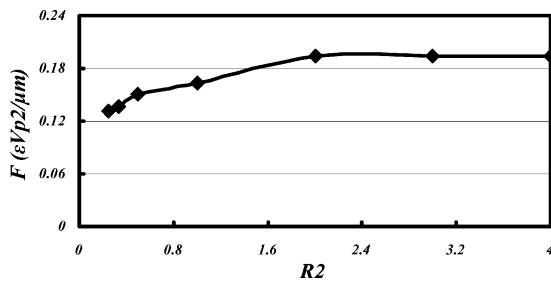


Fig. 13. The levitating force density (F) acting on the movable finger under diverse R_2 .

V. DISCUSSION

As we know, it is essential that both movable finger and fixed finger of in-plane interdigitated combdrive remain coplanar for high quality MEMS devices, so how to get the accurate electrostatic field and levitating force for levitation control is very important and indispensable for the design of MEMS devices. After using coarse mesh DBEM presented in this article to accurately calculate the electrostatic response of the comb finger biased with a dc voltage, the induced vertical force per unit length of the movable comb finger at different levitation positions can be obtained. Results show that the less the values of width ratio ($R_1 = w_m/w_f$) between movable and fixed fingers are, the larger the levitating force F acting on the movable finger is. In addition, the F becomes more dominant as the values of aspect ratio ($R_2 = h/w_m$) between the height h and width of fingers increases, but it will be kept constant while the R_2 becomes larger.

If the value of width of movable finger w_m is constant and the values of R_1 are variable, the values of normal electric field intensity $E_{n,2}$ on the upper side of movable finger are obviously dependent on the values of R_1 and the location to the left side of movable finger (loc), but the values of $E_{n,1}$ on the bottom side of movable finger are only apparently counting on the value of loc , and the effect of the values of R_1 can be ignored. If the values of R_2 are variable but the w_m is still kept constant, the fringing values of $E_{n,1}$ on the bottom and $E_{n,2}$ on the upper sides of movable finger are both obviously dependent on the values of R_2 and loc , but the effect of R_2 on other areas is not obvious.

By comparing the element mesh of refined mesh FEM and coarse mesh DBEM of electrostatic combdrive considering the fringing of field around the edges, one can see that numbers of elements and nodes for refined mesh FEM are much higher than those of coarse mesh DBEM to get a reasonable result. Though using FEM was widespread for MEMS device nowadays, it is still very difficult to establish the boundary conditions and generate the proper domain-type FEM because the values of finger width and aspect ratios (R_1 and R_2) for MEMS combdrive always change many times before final layout in the variable design stage. Therefore, we strongly recommend the boundary-type DBEM for studying the effect of finger width and aspect ratio variation for the levitation of MEMS combdrive because the DBEM's discretizations are restricted only to the

boundaries, and it is making data generation much easier than domain-type FEM.

VI. CONCLUSION

The dual integral formulation of electrostatic combdrive problems considering the fringing of field around the edges has been presented in this article. Comparisons of the results between FEM and DBEM analyzes were discussed with respect to diverse finger width and aspect ratios for electrostatic MEMS combdrive in order to demonstrate the efficiency of DBEM. It has been ensured that the capabilities of coarse mesh DBEM simulation are acceptable after comparison with the refined mesh FEM data. For electrical engineering practices, since the numbers of elements and nodes for refined mesh FEM are much higher than those of coarse mesh DBEM to get a reasonable result, and it wastes much time for diverse design if using the domain-type FEM, so the present boundary-type DBEM has great potential for industrial applications, especially in the initial variable design stage.

REFERENCES

- [1] W. C. Tang, T. C. H. Nguyen, M. W. Judy, and R. T. Howe, "Lateral driven polysilicon resonant microstructures," *Sens. Actuators*, vol. 20, pp. 25–32, 1989.
- [2] —, "Electrostatic-comb drive of lateral polysilicon resonators," *Sens. Actuators A, Phys.*, vol. A21-23, pp. 328–331, 1990.
- [3] W. C. Tang, M. G. Lim, and R. T. Howe, "Electrostatic comb drive levitation and control method," *J. Microelectromech. Syst.*, vol. 1, no. 4, pp. 170–178, Dec. 1992.
- [4] J. L. A. Yeh, C. Y. Hui, and N. C. Tien, "Electrostatic model for an asymmetric combdrive," *J. Microelectromech. Syst.*, vol. 9, no. 1, pp. 126–135, Mar. 2000.
- [5] W. A. Johnson and L. K. Warne, "Electrophysics of micromechanical comb actuators," *J. Microelectromech. Syst.*, vol. 4, no. 1, pp. 49–59, Mar. 1995.
- [6] W. Ye, S. Mukherjee, and N. C. MacDonald, "Optimal shape design of an electrostatic comb drive in microelectromechanical systems," *J. Microelectromech. Syst.*, vol. 7, no. 1, pp. 16–26, Mar. 1998.
- [7] D. K. Cheng, *Field and Wave Electromagnetics*. Reading, MA: Addison-Wesley, 1989.
- [8] U. Beerschwinger, N. G. Miline, S. J. Yang, R. L. Reuben, A. J. Sangster, and H. Ziad, "Coupled electrostatic and mechanical FEA of a micromotor," *J. Microelectromech. Syst.*, vol. 3, no. 4, pp. 162–171, Dec. 1994.
- [9] P. P. Silvester and F. L. Ferrari, *Finite Elements for Electrical Engineers*. Cambridge: Cambridge University Press, 1983.
- [10] J. Wiersig, "Boundary element method for resonances in dielectric microcavities," *J. Opt. A: Pure Appl. Opt.*, vol. 5, pp. 53–60, 2003.
- [11] S. D. Senturia, N. Aluru, and J. White, "Simulating the behavior of MEMS devices: Computational methods and needs," *IEEE Comput. Sci. Eng. Mag.*, pp. 30–43, Jan.–Mar. 1997.
- [12] J. T. Chen and H. K. Hong, "Review of dual boundary element methods with emphasis on hypersingular integrals and divergent series," *Trans. ASME, Appl. Mech. Rev.*, vol. 52, no. 1, pp. 17–33, 1999.
- [13] S. W. Chyuan, Y. S. Liao, and J. T. Chen, "An efficient method for solving electrostatic problems," *IEEE Comput. Sci. Eng. Mag.*, pp. 52–58, May–Jun. 2003.
- [14] J. T. Chen and S. R. Lin, "On the rank-deficiency problems in boundary integral formulation using the Fredholm alternative theory and singular value decomposition technique," in *Proc. Fifth World Congress on Computational Mechanics*, Vienna, Austria, July 7–12, 2002.
- [15] "I-DEAS user's guide," in *Finite Element Modeling*: SDRC, 1990.



Shiang-Woei Chyuan received the B.S. degree in naval architecture and marine engineering and the M.S. degree in aeronautical and astronautical engineering, from National Cheng Kung University, and the Ph.D. degree in mechanical engineering from the National Taiwan University, Taipei, Taiwan, R.O.C.

He is an Associate Scientist in the Missile and Rocket Systems Research Division, Chung Shan Institute of Science and Technology, Lung-Tan, Tao-Yuan, Taiwan, R.O.C. His technical interests include MEMS simulation and design, numerical

modeling and simulation of electrostatics and electromagnetics, and aging life analysis of solid-propellant grains.



Jeng-Tzong Chen received the B.S. degree in civil engineering, the M.S. degree in applied mechanics, and the Ph.D. degree in civil engineering from National Taiwan University, Taipei, Taiwan, R.O.C.

He is a Professor in the Department of Harbor and River Engineering National Taiwan Ocean University. His technical interests include computational mechanics, the boundary element method, and vibration and acoustics.



Yunn-Shiuan Liao received the M.S. and Ph.D. degrees in mechanical engineering from the University of Wisconsin-Madison.

He is a Professor and Director of Traditional and Nontraditional Machining in the Department of Mechanical Engineering at National Taiwan University. His research interests include nontraditional machining processes, the machining of difficult-to-cut materials, and precision machining.

Dr. Liao is a member of the American Society of Mechanical Engineers (ASME).